The golden ten equations of motion

EINDHOVEN UNIVERSITY OF TECHNOLOGY
Department of Mathematics and Computing Science

RANA 94-24
November 1994

The Golden Ten Equations of Motion

by

J.C. de Vos and A.A.F. van de Ven

Reports on Applied and Numerical Analysis
Department of Mathematics and Computing Science
Eindhoven University of Technology
P.O. Box 513
5600 MB Eindhoven
The Netherlands
ISSN: 0926-4507

The Golden Ten Equations of Motion

J.C. De Vos * A.A.F. Van de Ven **

November 18, 1994

1 Introduction

Golden Ten is a modified version of roulette. The game is played with a small ball moving in a relatively large bowl, at the bottom of which there is a ring with numbered compartments. The main differences with Roulette are that the drum is in fact a smooth, conic bowl, in which the ball is smoothly spiraling down, and secondly that the players do not have to stake before the ball has reached a certain level. Although the players can not effect the motion of the ball, it is claimed that the possibility to observe part of the ball's orbit enables them to make a better than random guess on the outcome, thus implying that Golden Ten is a game of skill, rather than a game of chance.

The main attributes of the game are a solid little ball, made of ivory-like synthetic material, and a big, slightly grooved, uncoated metal drum. Figs. 1 and 2 respectively contain a top- and a side-view of the drum. At the beginning of the game, the ball is launched from a slit plastic arm at the upper rim of the drum. After rolling a few rounds alongside of the rim, the ball gradually spirals down the drum, towards a ring with twenty-six numbered, equally large compartments. On the surface of the drum two concentric circles have been drawn (as shown in Fig. 1). The upper circle is called the observation ring, the lower one is the limit ring. The players start betting - on one or more possible outcomes - when the ball reaches the observation ring, and the betting must be stopped at the limit ring.

This paper employs a mechanical model to describe the motion of the ball in the drum. The result of this model is a set of differential equations. Provided that the values of the physical constants in the model are known, this set of equations can be solved numerically. The friction coefficients generate a problem here, because they have to be estimated by means of complementary experiments. After the numerical solution has been presented, the paper proceeds with a quest for an analytical solution. The system of equations is rewritten in terms of a set of small parameters - implicitly representing the friction coefficients and the drum's angle of inclination - and an analytical method is employed to express the solution as an asymptotic power series. A part of the solution will even be determined exactly. At the end of the paper, the attained results will be

*Co-operation Centre Tilburg and Eindhoven Universities, P.O. box 90153, 5000 LE Tilburg
**Eindhoven University of Technology, P.O. box 513, 5600 MB Eindhoven

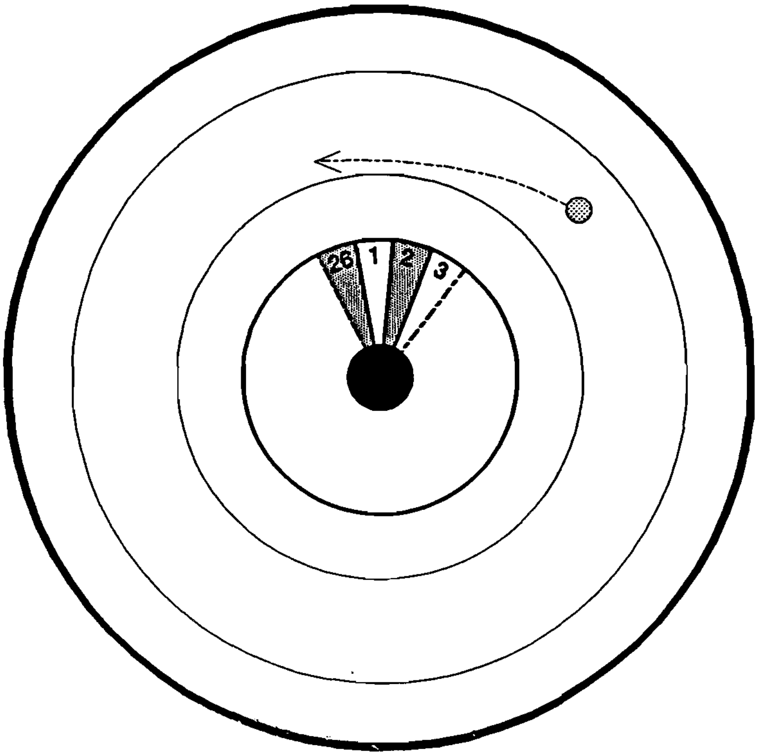

Figure 1: The Golden Ten drum; top-view.

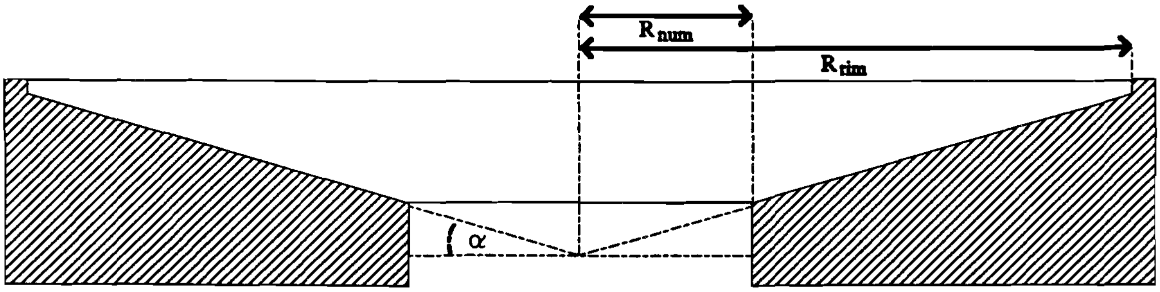

Figure 2: The Golden Ten drum; side-view.

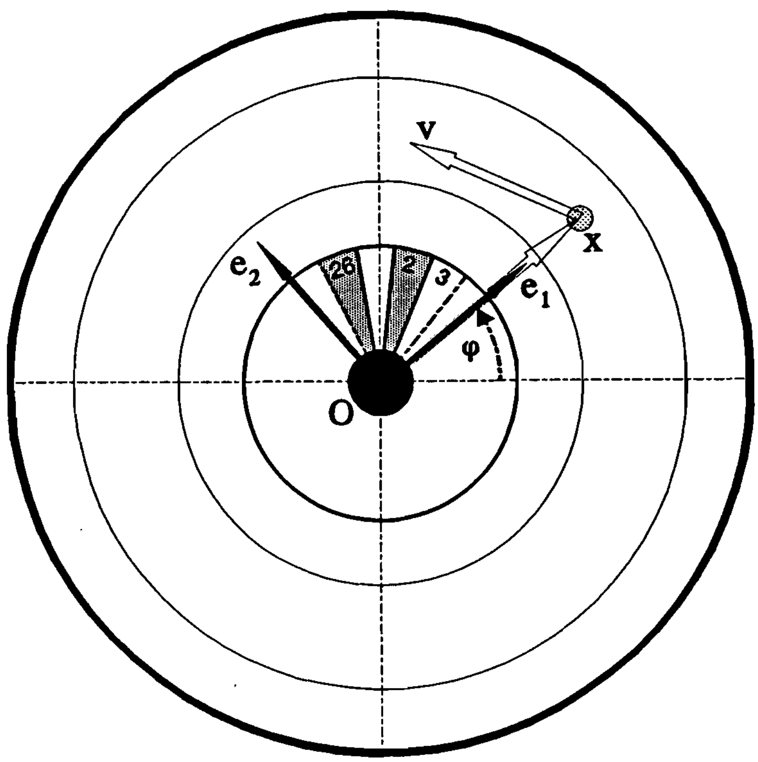

Figure 3: The moving frame $\{O\mathbf{e}_1\mathbf{e}_2\mathbf{e}_3\}$; top-view.

utilized to predict the outcome of the game. The paper concludes with some suggestions and directives for further research.

2 The mechanical model

The most natural model to describe the motion of the ball is a three dimensional rigid body model, but before such a model can be constructed, we have to make some basic assumptions:

i) the ball is considered to be a uniform sphere;

ii) the drum is assumed to be rotationally symmetric;

iii) the surface of the drum - including that of the rim - is considered to be so smooth that the ball rolls without bouncing, but (on the other hand) so rough that the ball - after two or three revolutions along the rim - rolls without slipping;

iv) the motion of the ball is completely deterministic, i.e. no random factors are included.

No assumptions are made for the, preferably, horizontal position of the drum, i.e. we allow for a slightly tilted position. We denote the angle over which the drum is tilted with β. The radius of the ball is a, that of the rim is R_{rim}, whereas R_{num} denotes the radius of the numbered ring. The angle of inclination of the conical drum surface is α (as in Fig. 2). Note that $0 < \alpha \ll \pi/2$ and $0 \leq \beta \ll \alpha$.

A moving rectangular coordinate system $\{O\mathbf{e}_1\mathbf{e}_2\mathbf{e}_3\}$ is introduced to describe the motion of the ball on the drum surface (see Figs. 3 and 4). Here, the origin O coincides

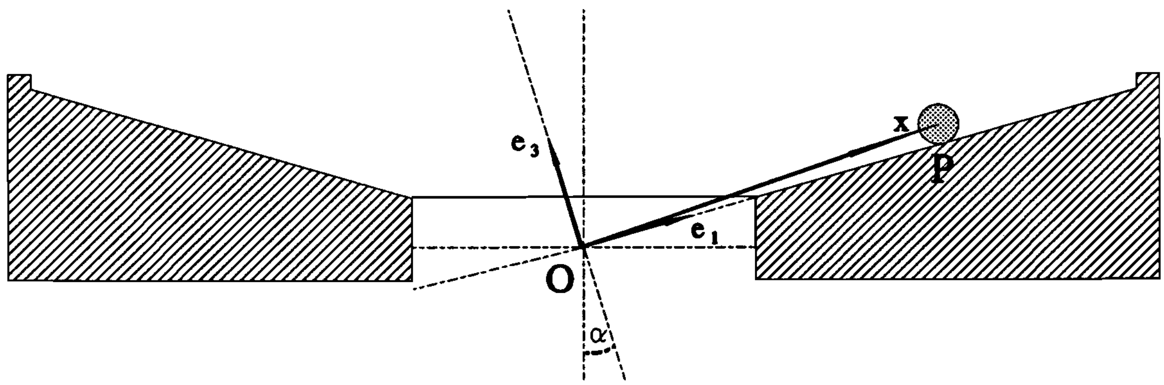

Figure 4: The moving frame $\{O\mathbf{e}_1\mathbf{e}_2\mathbf{e}_3\}$; side-view.

with the apex of the drum, $\boldsymbol{e}_1$ points in the direction from O to P - being the point of contact between the ball and the drum - and $\boldsymbol{e}_3$ is parallel to the drum surface normal in P. Calling φ the angle of rotation of $\boldsymbol{e}_1$ about the central axis of the drum, we obtain for the angular velocity $\boldsymbol{\Omega}$ of the $\{O\boldsymbol{e}_1\boldsymbol{e}_2\boldsymbol{e}_3\}$ frame:

$$\boldsymbol{\Omega} = \dot{\varphi}\sin\alpha\boldsymbol{e}_1 + \dot{\varphi}\cos\alpha\boldsymbol{e}_3. \tag{1}$$

The rotation of the coordinate axes can thus be written as

$$\dot{\boldsymbol{e}}_i = \boldsymbol{\Omega} \times \boldsymbol{e}_i. \tag{2}$$

The position $\boldsymbol{x}_o$ of the centre of the ball o, with respect to O, can be written as

$$\boldsymbol{x}_o = r\boldsymbol{e}_1 + a\boldsymbol{e}_3, \tag{3}$$

where r is the distance from O to P. The velocity $\boldsymbol{v}_o$ of o is the time derivative of $\boldsymbol{x}_o$, so it equals

$$\boldsymbol{v}_o = \dot{\boldsymbol{x}}_o = \dot{r}\boldsymbol{e}_1 + r\dot{\boldsymbol{e}}_1 + a\dot{\boldsymbol{e}}_3. \tag{4}$$

By substituting (2) into (4), and introducing

$$R = r\cos\alpha - a\sin\alpha, \tag{5}$$

we obtain

$$\begin{aligned} \boldsymbol{v}_o &= \dot{r}\boldsymbol{e}_1 + (r\dot{\varphi}\cos\alpha - a\dot{\varphi}\sin\alpha)\boldsymbol{e}_2 \\ &= \frac{\dot{R}}{\cos\alpha}\boldsymbol{e}_1 + R\dot{\varphi}\boldsymbol{e}_2. \end{aligned} \tag{6}$$

Likewise, the acceleration of o is

$$\begin{aligned} \dot{\boldsymbol{v}}_o &= \frac{\ddot{R}}{\cos\alpha}\boldsymbol{e}_1 + \frac{\dot{R}}{\cos\alpha}\dot{\boldsymbol{e}}_1 + \dot{R}\dot{\varphi}\boldsymbol{e}_2 + R\ddot{\varphi}\boldsymbol{e}_2 + R\dot{\varphi}\dot{\boldsymbol{e}}_2 \\ &= (\frac{\ddot{R}}{\cos\alpha} - R\dot{\varphi}^2\cos\alpha)\boldsymbol{e}_1 + (R\ddot{\varphi} + 2\dot{R}\dot{\varphi})\boldsymbol{e}_2 + R\dot{\varphi}^2\sin\alpha\boldsymbol{e}_3. \end{aligned} \tag{7}$$

According to assumption iii, the ball purely rolls, hence the instantaneous velocity $\boldsymbol{v}_P$ of P is zero. With $\boldsymbol{\omega}$ denoting the angular velocity of the ball, this implies

$$\mathbf{o} = \boldsymbol{v}_P = \boldsymbol{v}_o + \boldsymbol{\omega} \times (-a\boldsymbol{e}_3). \tag{8}$$

Substitution of (6) into (8) yields

$$\boldsymbol{\omega} = -\frac{R\dot{\varphi}}{a}\boldsymbol{e}_1 + \frac{\dot{R}}{a\cos\alpha}\boldsymbol{e}_2 + \dot{\psi}\boldsymbol{e}_3, \tag{9}$$

where $\dot{\psi}$ denotes the third component of $\boldsymbol{\omega}$. We will call this third component the *spin*. The time derivative of $\boldsymbol{\omega}$ follows from differentiating (9) and substituting (2) into the result, i.e.

$$\begin{aligned} \dot{\boldsymbol{\omega}} &= -\frac{\dot{R}\dot{\varphi} + R\ddot{\varphi}}{a}\boldsymbol{e}_1 - \frac{R\dot{\varphi}}{a}\dot{\boldsymbol{e}}_1 + \frac{\ddot{R}}{a\cos\alpha}\boldsymbol{e}_2 + \frac{\dot{R}}{a\cos\alpha}\dot{\boldsymbol{e}}_2 + \ddot{\psi}\boldsymbol{e}_3 + \dot{\psi}\dot{\boldsymbol{e}}_3 \\ &= -\frac{R\ddot{\varphi} + 2\dot{R}\dot{\varphi}}{a}\boldsymbol{e}_1 + (\frac{\ddot{R} - R\dot{\varphi}^2\cos^2\alpha}{a\cos\alpha} - \dot{\varphi}\dot{\psi}\sin\alpha)\boldsymbol{e}_2 + (\frac{\dot{R}\dot{\varphi}\tan\alpha}{a} + \ddot{\psi})\boldsymbol{e}_3. \end{aligned} \tag{10}$$

The equations of motion are implicitly contained in the law of momentum and that of moment of momentum. With m representing the mass of the ball, and $\boldsymbol{F}$ the total force acting on the ball, the first law reads

$$m\dot{\boldsymbol{v}}_o = \boldsymbol{F}, \tag{11}$$

and the second states

$$I\dot{\boldsymbol{\omega}} = \boldsymbol{M}, \tag{12}$$

with I being the central moment of inertia, so $I = \frac{2}{5}ma^2$, and $\boldsymbol{M}$ being the momentum about o. Before we can elaborate these equations - by writing them out in components with respect to the $\{O\boldsymbol{e}_1\boldsymbol{e}_2\boldsymbol{e}_3\}$ system - we first must specify $\boldsymbol{F}$ and $\boldsymbol{M}$. Four distinct forces act on the ball: the normal force $\boldsymbol{F}_n$, the frictional force (or dry friction) $\boldsymbol{F}_d$, the resistive force $\boldsymbol{F}_a$ (due to air friction) and the gravitational force $\boldsymbol{F}_g$. These forces combine into

$$\boldsymbol{F}_n + \boldsymbol{F}_d + \boldsymbol{F}_a + \boldsymbol{F}_g = \boldsymbol{F}. \tag{13}$$

We note that the forces $\boldsymbol{F}_n$, $\boldsymbol{F}_a$ and $\boldsymbol{F}_g$ act in o, whereas the line of action of $\boldsymbol{F}_d$ is through P. Hence, only $\boldsymbol{F}_d$ contributes to the moment about o.

The normal force can simply be written as

$$\boldsymbol{F}_n = N\boldsymbol{e}_3, \tag{14}$$

where N is a nonnegative scalar. Likewise, the frictional force, which is tangent to the surface of the drum in P, is given by

$$\boldsymbol{F}_d = D_1\boldsymbol{e}_1 + D_2\boldsymbol{e}_2. \tag{15}$$

The resistive force $\boldsymbol{F}_a$ is due to the air friction the ball experiences on account of the translation. Since this force is directed opposite to $\boldsymbol{v}_o$, and its magnitude depends on v_o, we write

$$\begin{aligned} \boldsymbol{F}_a &= -mf(v_o)\boldsymbol{v}_o \\ &= -mf(v_o)(\frac{\dot{R}}{\cos\alpha}\boldsymbol{e}_1 + R\dot{\varphi}\boldsymbol{e}_2), \end{aligned} \tag{16}$$

where

$$v_o = \|\boldsymbol{v}_o\| = \sqrt{\frac{\dot{R}^2}{\cos^2\alpha} + R^2\dot{\varphi}^2}, \tag{17}$$

and $f(v_o)$ is assumed to be a simple function of v_o, e.g. a constant or a linear function. For the gravitational force, we know that it would be directed along the central axis of the drum, if the position of the drum was exactly horizontal (the ideal case). Since we here assume that the drum is tilted about a small angle β, and that the plane of inclination is rotated about an angle φ_β ($\varphi_\beta \in [0, 2\pi)$), we now have that $\boldsymbol{F}_g$ takes the form

$$\begin{aligned} \boldsymbol{F}_g = &- mg(\cos\alpha\sin\beta\cos(\varphi-\varphi_\beta) + \sin\alpha\cos\beta)\ \boldsymbol{e}_1 \\ &+ mg\sin\beta\sin(\varphi-\varphi_\beta)\ \boldsymbol{e}_2 \\ &+ mg(\sin\alpha\sin\beta\cos(\varphi-\varphi_\beta) - \cos\alpha\cos\beta)\ \boldsymbol{e}_3, \end{aligned} \tag{18}$$

where g respresents the acceleration of gravity.

The last term to express in $\{\boldsymbol{e}_1\boldsymbol{e}_2\boldsymbol{e}_3\}$ coordinates is the total moment $\boldsymbol{M}$. $\boldsymbol{M}$ is composed of two parts: the rolling resistance $\boldsymbol{M}_r$, which is assumed to be proportional to the spin (rolling resistance due to the in-plane rotations ω_1 and ω_2 is neglected), and the moment $\boldsymbol{M}_d$, which is caused by the frictional force $\boldsymbol{F}_d$. Hence

$$\boldsymbol{M} = \boldsymbol{M}_d + \boldsymbol{M}_r, \tag{19}$$

with

$$\boldsymbol{M}_d = -a\boldsymbol{e}_3 \times \boldsymbol{F}_d = aD_2\boldsymbol{e}_1 - aD_1\boldsymbol{e}_2, \tag{20}$$

and

$$\boldsymbol{M}_r = -Nh\dot{\psi}\boldsymbol{e}_3, \tag{21}$$

where h is a friction coefficient. From (3), (6) and (9), we know that the motion of the ball is completely determined by the three variables R, φ and $\dot{\psi}$. By writing (11) and (12) out in components in the $\{O\boldsymbol{e}_1\boldsymbol{e}_2\boldsymbol{e}_3\}$ system, and by eliminating the unknowns N, D_1 and D_2, we obtain

$$\begin{aligned} \ddot{R} &= -\tfrac{5}{7}f(v_o)\dot{R} + R\dot{\varphi}^2\cos^2\alpha + \tfrac{a}{7}\dot{\varphi}\dot{\psi}\sin(2\alpha) - \tfrac{5g}{7}\cos^2\alpha(\sin\beta\cos(\varphi-\varphi_\beta) + \tan\alpha\cos\beta) \\ \ddot{\varphi} &= -\tfrac{5}{7}f(v_o)\dot{\varphi} - 2\frac{\dot{R}\dot{\varphi}}{R} + \tfrac{5g}{7}\tfrac{1}{R}\sin\beta\sin(\varphi-\varphi_\beta) \\ \ddot{\psi} &= -\tfrac{5h}{2a^2}\dot{\psi}\{R\dot{\varphi}^2\sin\alpha - g(\sin\alpha\sin\beta\cos(\varphi-\varphi_\beta) - \cos\alpha\cos\beta)\} - \tfrac{1}{a}\dot{R}\dot{\varphi}\tan\alpha\ . \end{aligned} \tag{22}$$

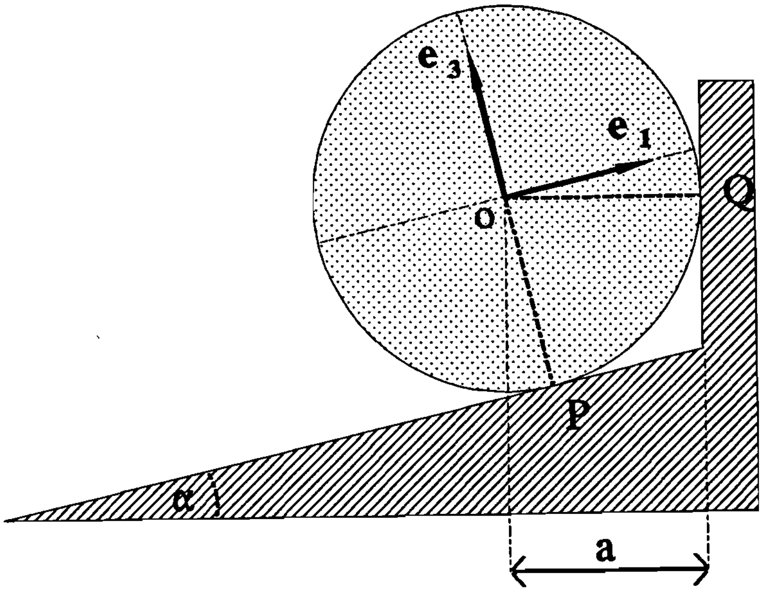

Figure 5: The ball rolling along the rim.

The above system of differential equations can only be solved when complemented with a set of initial conditions. We derive these conditions by again using assumption iii: when the ball is rolling along the rim, we know (see Fig. 5) that the instantaneous velocity $\boldsymbol{v}_Q$ of Q - being the point of contact between rim and ball - must be zero. So

$$\mathbf{o} = \boldsymbol{v}_Q = \boldsymbol{v}_o + \boldsymbol{\omega} \times a(\cos\alpha \boldsymbol{e}_1 - \sin\alpha \boldsymbol{e}_3). \tag{23}$$

By substitution of equations (6) and (9) into (23), we find

$$\frac{\dot{R}(1-\sin\alpha)}{\cos\alpha}\boldsymbol{e}_1 + \{a\dot{\psi}\cos\alpha + R\dot{\varphi}(1-\sin\alpha)\}\boldsymbol{e}_2 - \dot{R}\boldsymbol{e}_3 = \mathbf{o}. \tag{24}$$

Let the initial time $t = 0$ be the time when the ball leaves the rim. From (24) we conclude that, at $t = 0$, the ball momentarily moves in a circular orbit ($\ddot{R} = \dot{R} = 0$), with radius $R(0) = R_{rim} - a$. Furthermore, since we are only interested in the relative difference between the point where the ball leaves the rim and that where it ultimately hits the numbered ring, we may choose $\varphi(0)$ arbitrarily, so we have $\varphi(0) = \varphi_0$. To find $\dot{\varphi}(0)$ and $\dot{\psi}(0)$, we combine the second term in (24) with the first equation in (22), whence

$$\begin{aligned} R(0) &= R_{rim} - a, & \dot{R}(0) &= 0, \\ \varphi(0) &= \varphi_0, & \dot{\varphi}(0) &= \sqrt{\frac{5g(\sin\alpha\cos\beta + \cos\alpha\sin\beta\cos(\varphi_0 - \varphi_\beta))}{R(0)(7\cos\alpha - 2\tan\alpha(1-\sin\alpha))}}\ . \\ \dot{\psi}(0) &= R(0)\dot{\varphi}(0)\tfrac{\sin\alpha - 1}{a\cos\alpha}\ , \end{aligned} \tag{25}$$

At this point, we have derived a system of three nonlineair second order differential equations (22), with a proper set of initial conditions (25). This system completely determines the motion of the ball in the drum, but unfortunately it does not allow for any standard analytical solution method.

3 Numerical solutions

Any system of second order differential equations can be rewritten as a system of first order differential equations by introducing some extra variables. To this end, we define

$$x_1 = R,\ x_2 = \dot{R},\ x_3 = \varphi - \varphi_\beta,\ x_4 = \dot{\varphi},\ x_5 = \dot{\psi}, \tag{26}$$

and regard these variables as components of the five-vector

$$\boldsymbol{x}(t) = (x_1(t), x_2(t), x_3(t), x_4(t), x_5(t)). \tag{27}$$

With these new variables, the equations of motion (22) can be rewritten as

$$\begin{aligned}
\dot{x}_1 &= x_2 \\
\dot{x}_2 &= -\tfrac{5}{7}f(v_o)x_2 + x_1{x_4}^2\cos^2\alpha + \tfrac{a}{7}x_4x_5\sin(2\alpha) - \tfrac{5g}{7}(\cos x_3\sin\beta + \tan\alpha\cos\beta)\cos^2\alpha \\
\dot{x}_3 &= x_4 \\
\dot{x}_4 &= -\tfrac{5}{7}f(v_o)x_4 - 2\tfrac{x_2x_4}{x_1} + \tfrac{5g}{7}\tfrac{\sin x_3}{x_1}\sin\beta \\
\dot{x}_5 &= -\tfrac{5h}{2a^2}x_5\{x_1{x_4}^2\sin\alpha + g(\cos x_3\sin\alpha\sin\beta - \cos\alpha\cos\beta)\} - \tfrac{1}{a}x_2x_4\tan\alpha,
\end{aligned} \tag{28}$$

where

$$v_o = \sqrt{{x_1}^2{x_4}^2 + \frac{{x_2}^2}{\cos^2\alpha}}. \tag{29}$$

Likewise, with

$$x_{0i} = x_i(0), \tag{30}$$

the initial conditions (25) can be transformed into

$$\begin{aligned}
x_{01} &= R_{rim} - a \\
x_{02} &= 0 \\
x_{03} &= 0 \\
x_{04} &= \sqrt{\tfrac{5g(\sin\alpha\cos\beta + \cos\alpha\sin\beta)}{(7\cos\alpha - 2\tan\alpha(1-\sin\alpha))x_{01}}} \\
x_{05} &= -\tfrac{1-\sin\alpha}{a\cos\alpha}x_{01}x_{04}\ ,
\end{aligned} \tag{31}$$

where the value of $\varphi_0 - \varphi_\beta$ is, for the sake of simplicity, set to zero. The system of differential equations is now written in the formal representation

$$\frac{d\boldsymbol{x}(t)}{dt} = \boldsymbol{f}(\boldsymbol{x}(t)), \tag{32}$$

with initial conditions

$$\boldsymbol{x}(0) = \boldsymbol{x}_o. \tag{33}$$

We can solve this type of differential equations by using a Runge-Kutta method, but before we can run such a routine, we have to fill in the numerical values of the system parameters in both (28) and (31).

When the game is played under ideal circumstances (i.e. with a perfectly horizontal position of the drum), we have

$$\beta = \varphi_\beta = 0. \tag{34}$$

The dimensions of the drum and the ball are supplied by [De Vos 1994], from which we obtain

$$a = 0.0175\ (m),\ R_{rim} = 0.487\ (m),\ R_{num} = 0.205\ (m),\ \alpha = 0.083\ (rad). \tag{35}$$

For the acceleration of gravity we have

$$g = 9.807\ (m/sec^2). \tag{36}$$

The values according to (34)-(36) lead to the following initial conditions

$$x_{01} = 0.470\ (m),\ x_{02} = x_{03} = 0,\ x_{04} = 1.13\ (rad/sec),\ x_{05} = -28\ (rad/sec), \tag{37}$$

or, as a vector,

$$\boldsymbol{x}_o = (0.470, 0, 0, 1.13, -28). \tag{38}$$

This leaves us with the unknown friction coefficient h and the unknown friction function f. In first instance, we neglect the resistive force due to spin, implying

$$h = 0. \tag{39}$$

For the air resistance we have two simple options: the resistive force can be assumed to be directly proportional to the speed v_o, in which case

$$f(v_o) = f_l, \tag{40}$$

or we can postulate a pure quadratic model, implying

$$f(v_o) = f_s v_o. \tag{41}$$

We tentatively consider these models to be equally acceptible, so we will - until further notice - employ them both. At the final time t_f, when the ball hits the numbered ring, we have

$$x_1(t_f) = R_{num}, \tag{42}$$

which provides us with an extra condition for x_1. The value of t_f can be estimated by using the experimental data supplied by [De Vos 1994]. From orbit T11B21 - which is one of the smoothest orbits, and therefore will serve as an example - we obtain the value

$$\widehat{t_f} = 116\ (sec). \tag{43}$$

We can now determine the two coefficients f_l and f_s by running two Runge-Kutta procedures (one for each friction model) for varying values of f_l and f_s, while continually checking on condition (42), with t_f substituted by $\widehat{t_f}$. This method eventually yields the rough estimates

$$\begin{aligned} \widehat{f_l} &= 0.015\,(sec^{-1}), \qquad (44)\\ \widehat{f_s} &= 0.035\,(m^{-1}). \qquad (45) \end{aligned}$$

With the above data we have run the Runge-Kutta routine ODE45.M, supplied by the mathematical software package 386-MATLAB©, where we set the error tolerance to 10^{-6}. The results are reported in Figs. 6-11, where the dashed graphs represent the output from the quadratic friction model. Fig. 6 shows an almost linearly evolving total covered angle φ, for both models. Therefore, and because the motion of the ball is in fact an orbit round the centre of the drum, we will often consider the solution as a function of φ, rather than of t. A more natural way to observe the motion of the ball, especially from a player's point of view, is thus depicted in Fig. 7. It shows that the ball slowly spirals down the drum, with clearly perceptible elliptical revolutions. The

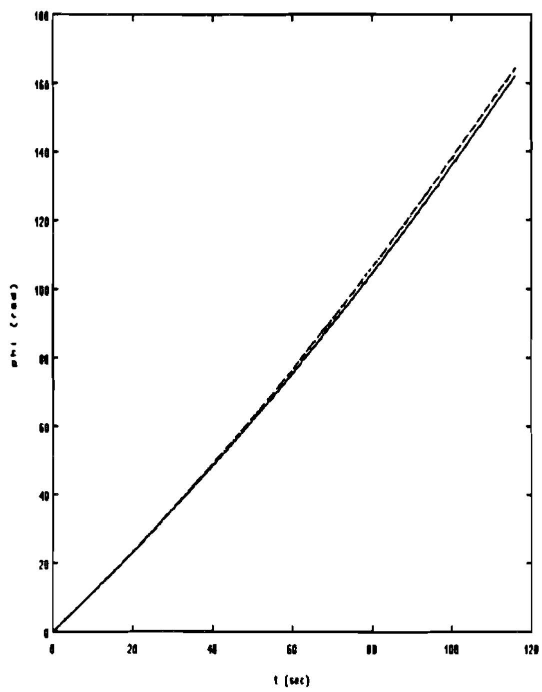

Figure 6: Total covered angle φ as function of time t.

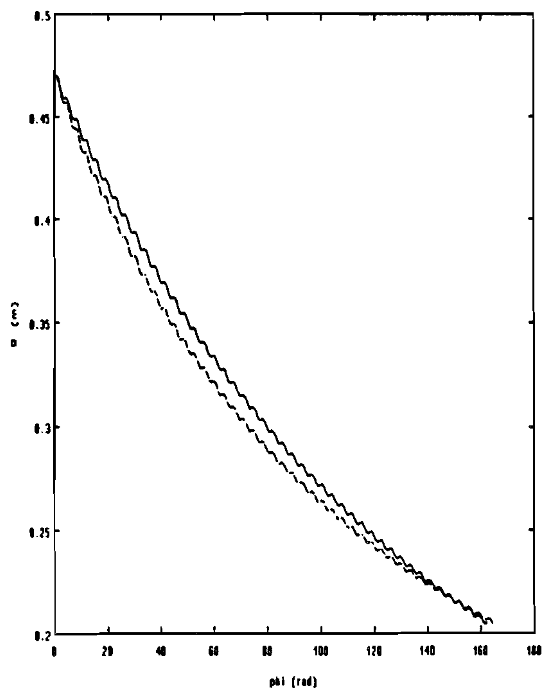

Figure 7: Radius R as function of φ.

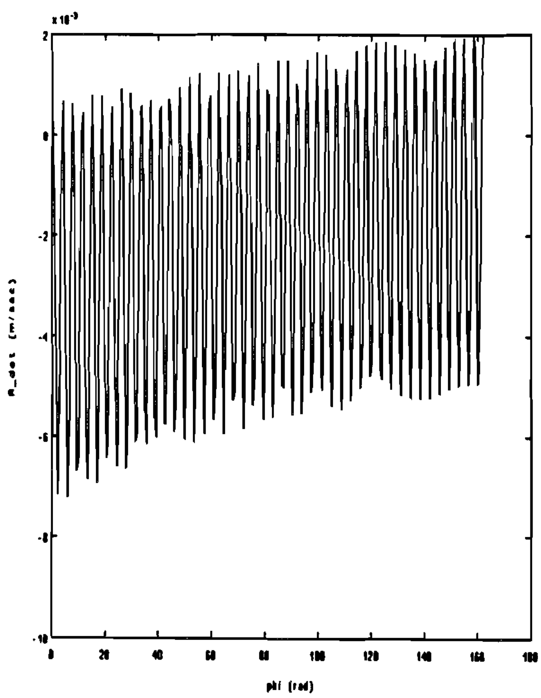

Figure 8: Radial velocity $\dot{R}$ as function of φ (linear model).

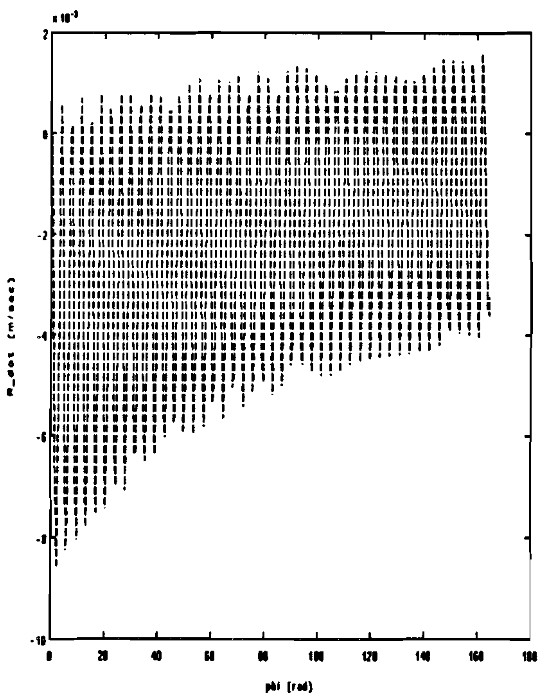

Figure 9: Radial velocity R as function of φ (quadratic model).

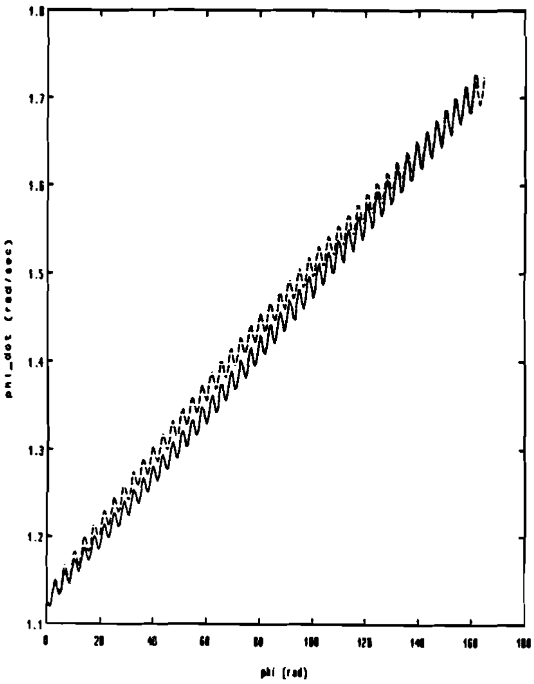

Figure 10: Angular velocity $\dot{\varphi}$ as function of φ.

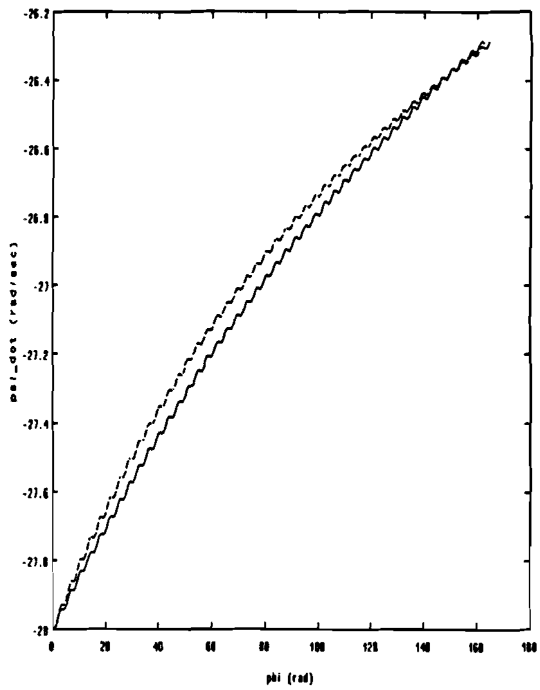

Figure 11: Spin $\dot{\psi}$ as function of φ.

distance to the centre of the drum decreases slightly faster in the quadratic case, as do the corresponding oscillations (see Figs. 8 and 9). The angular velocity of the ball shows a gradual increase, whereas the spin gradually decreases (see Figs. 10 and 11). Although the two friction models lead to different results, the overall characteristics appear to be very similar. We prefer to work with the linear model. Our reasons for this preference will be stated in the next section.

4 Analytical solutions

In this section - as in the previous section - we neglect the spinning resistance, and assume that the drum is in a perfectly horizontal position. Hence the motion of the ball primarily depends on the resistive force due to air friction. In order to bring an analytical approach within reach, we somewhat simplify the model by assuming that the resistive force $\boldsymbol{F}_a$ is a linear, rather than a quadratic, function of the speed $\boldsymbol{v}_o$. The consequences of this are discussed later on in this section (in connection with Fig. 13). By our assumptions, system (22) simplifies to

$$
\begin{aligned}
\ddot{R} &= -\tfrac{5}{7}f_l\dot{R} + R\dot{\varphi}^2\cos^2\alpha + (\tfrac{2a}{7}\dot{\varphi}\dot{\psi} - \tfrac{5g}{7})\sin\alpha\cos\alpha \\
\ddot{\varphi} &= -(\tfrac{5}{7}f_l + 2\tfrac{\dot{R}}{R})\dot{\varphi} \qquad\qquad (46) \\
\ddot{\psi} &= -\tfrac{1}{a}\dot{R}\dot{\varphi}\tan\alpha\,.
\end{aligned}
$$

When air resistance is completely neglected ($f(v_o) = f_l = 0$), the equations of motion admit three first integrals, representing conservation of angular momentum - about two distinct axes - and of energy.

4.1 An exact solution

When $f_l = 0$, the equations in (46) reduce to

$$\begin{aligned} \ddot{R} &= R\dot{\varphi}^2\cos^2\alpha + (\frac{2a}{7}\dot{\varphi}\dot{\psi} - \frac{5g}{7})\sin\alpha\cos\alpha, && (47)\\ \ddot{\varphi} &= -2\frac{\dot{R}}{R}\dot{\varphi}, && (48)\\ \ddot{\psi} &= -\frac{1}{a}\dot{R}\dot{\varphi}\tan\alpha. && (49) \end{aligned}$$

From (48) we find that

$$\frac{d}{dt}\{R^2\dot{\varphi}\} = 0, \tag{50}$$

reflecting conservation of angular momentum about the central axis of the drum. Combination of (48) and (49) leads to conservation of angular momentum about the axis of spin, or

$$\frac{d}{dt}\{\acute{a}^2\dot{\psi} - aR\dot{\varphi}\tan\alpha\} = 0. \tag{51}$$

Another quantity that is preserved in the absence of air friction is the total energy, being the sum of kinetic and potential energy. From equations (47) to (49) we can deduce

$$\frac{d}{dt}\{\frac{7m}{10}(\frac{\dot{R}^2}{\cos\alpha^2} + R^2\dot{\varphi}^2) + \frac{ma^2}{5}\dot{\psi}^2 + mgR\tan\alpha\} = 0. \tag{52}$$

Hence, the most direct way to study the dependency on coefficient f_l is by analyzing the momentary changes in the three physical quantities in equations (50) to (52).

To this end, let us consider the new variables

$$y_1' = R^2\dot{\varphi},\ y_2' = a\dot{\psi} - R\dot{\varphi}\tan\alpha. \tag{53}$$

After differentiation we find

$$\begin{aligned} \dot{y}_1' &= -\frac{5}{7}f_l y_1', && (54)\\ \dot{y}_2' &= -\frac{5}{7}f_l\frac{y_1'}{R}\tan\alpha. && (55) \end{aligned}$$

A full system of differential equations can be obtained by completing this set of variables with R. Note that expression (52) will not be used here, since it will needlessly complicate the calculations. After standardizing the variables to initial values 1 and 0, we obtain three new variables

$$y_1 = \frac{R^2\dot{\varphi}}{R(0)^2\dot{\varphi}(0)},\ y_2 = \frac{a\dot{\psi} - R\dot{\varphi}\tan\alpha}{a\dot{\psi}(0) - R(0)\dot{\varphi}(0)\tan\alpha},\ y_3 = \frac{R}{R(0)}, \tag{56}$$

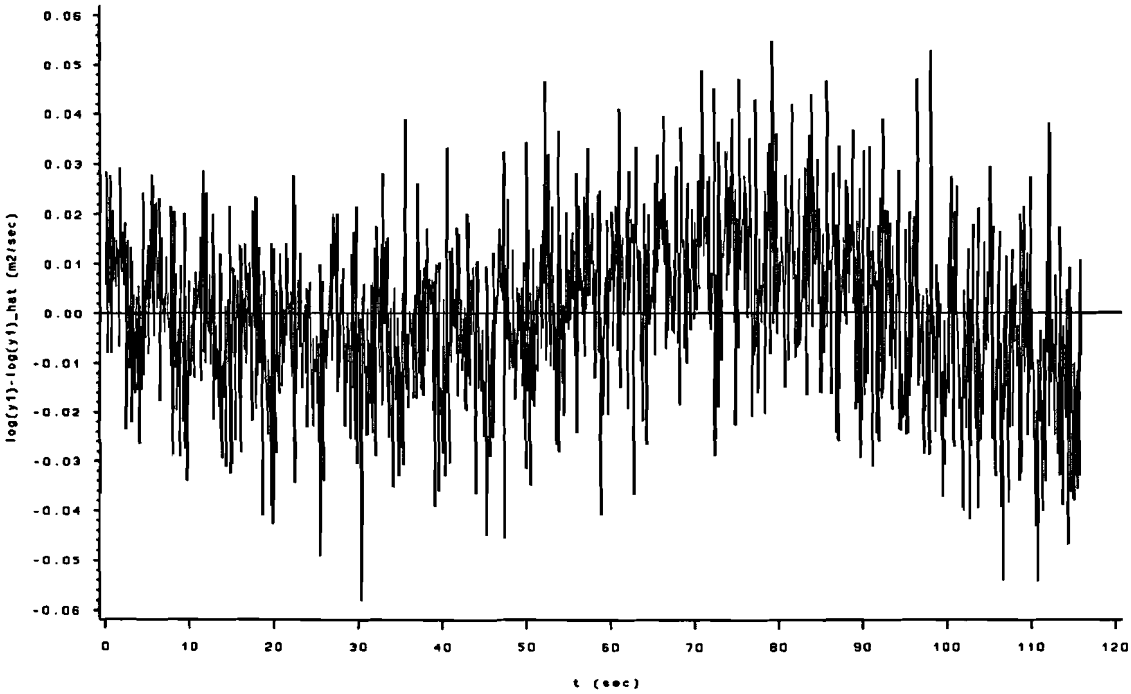

Figure 12: Regression residuals

and a system of nonlinear differential equations

$$
\begin{aligned}
\dot{y}_1 &= -\tfrac{5}{7} f_l y_1 \\
\dot{y}_2 &= -\tfrac{5}{7} f_l \tfrac{y_1}{y_3} \sin\alpha \qquad (57)\\
\ddot{y}_3 &= -\tfrac{5}{7} f_l \dot{y}_3 + \tfrac{5g}{7R(0)}\left(\tfrac{7-5\sin^2\alpha}{7-2\sin\alpha-5\sin^2\alpha}\frac{y_1{}^2}{y_3{}^2} - \tfrac{2\sin\alpha}{7-2\sin\alpha-5\sin^2\alpha}\frac{y_1 y_2}{y_3{}^2} + 1\right)\sin\alpha\cos\alpha\,,
\end{aligned}
$$

with initial conditions

$$
\begin{aligned}
y_1(0) = y_2(0) = y_3(0) &= 1 \\
\dot{y}_3(0) &= 0\,.
\end{aligned}
\qquad (58)
$$

The first equation in (57) is uncoupled from the rest of the system, and leads - through the corresponding initial condition in (58) - to the solution

$$
y_1 = e^{-\frac{5}{7} f_l t}. \qquad (59)
$$

This formula expresses the explicit dependency of the total covered area per unit time $R^2\dot{\varphi}$ on the air friction coefficient f_l and time t. It does however not provide separate formulas for any of the basic variables R, φ, or $\dot{\psi}$.

4.2 An estimated solution

By fitting equation (59) to the experimental data provided by [De Vos 1994], we can expect to obtain a more accurate estimate of coefficient f_l than in (44). A logarithmic

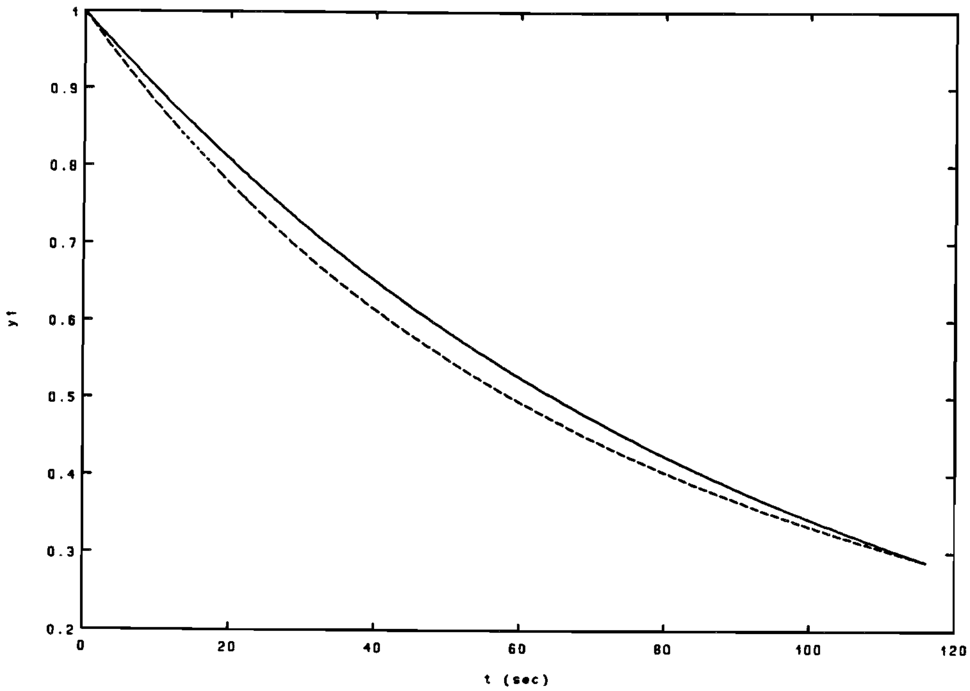

Figure 13: Total covered area per unit time $R^2\dot{\varphi}$ as function of t.

transformation and a simple linear regression model, applied to orbit T11B21, yield the estimated value

$$\widehat{f_l} = 0.014\ (sec^{-1}). \tag{60}$$

Note that this value differs only slightly to the one in (44). Fig. 12 shows the residuals from the regression model. The apparently small residuals indicate a close fit, but the rough sine shape does not indicate a truely linear friction model. But it also does not point to a truely quadratic model, as can be seen in Fig. 13, where we used the earlier estimates of f_l and f_s to plot y_1 for both friction models (the dashed line respresents the quadratic model). Because of its elegance and greater simplicity, we favour the linear model.

Substitution of the estimated f_l in (60) into the Runge-Kutta procedure does not lead to an orbit that closely matches example orbit T11B21. One of the obvious reasons for this is that the experimentally determined initial angular velocity appears to be lower than the theoretical value of 1.13 (rad/sec) in (37). [De Vos 1994] reports the value

$$\widehat{\dot{\varphi}(0)} = 1.09\ (rad/sec). \tag{61}$$

Fig. 14 compares orbit T11B21 to the Runge-Kutta output based on the newly estimated values of f_l and $\dot{\varphi}(0)$ (the dashed graph represents the Runge-Kutta output). The overall shape of the graphs appears to be quite similar, especially during the first part of the experiment. However, the second part shows a slightly varying phase shift and a small variation in amplitude. For a closer match we obviously need an extended model. The influence of the system parameters and the initial conditions on the orbit of the ball can be better judged when system (46) is supplied with an analytical solution. Since such a solution is not available, we are confined to an asymptotic solution. In the next subsection, we will present such a solution. The asymptotics are based on the small values of f_l and α.

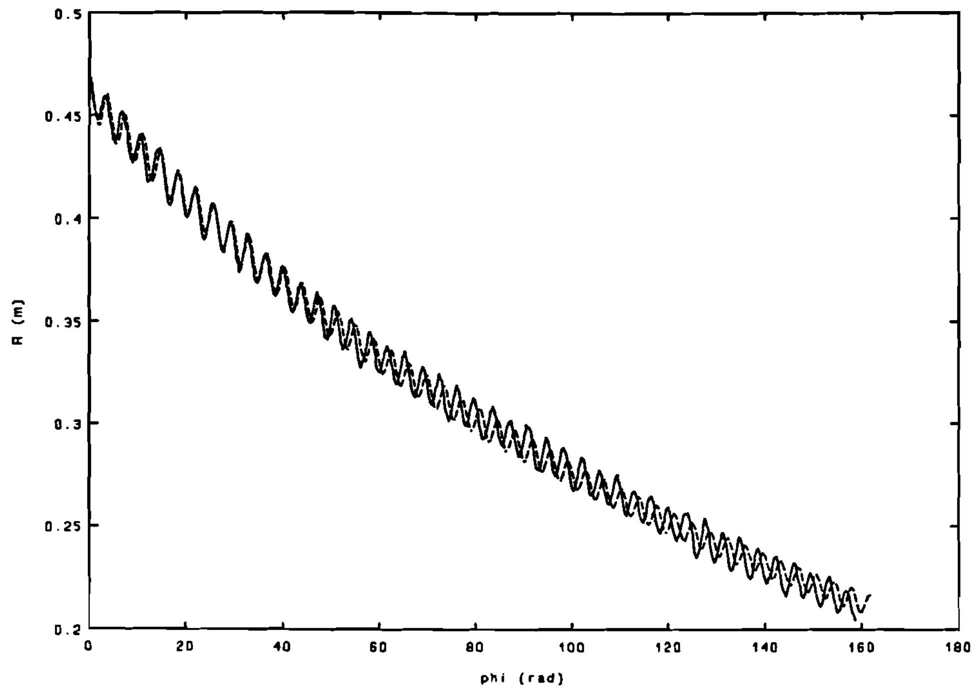

Figure 14: A comparison of numerical results and experimental data

4.3 Asymptotic solutions

Since the motion of the ball is an orbit round the centre of the drum, it is only natural to replace independent variable t in system (57) with variable φ. From the definitions in (56) we immediately find

$$\frac{d\varphi}{dt} = \dot{\varphi} = \dot{\varphi}(0)\frac{y_1}{u^2}, \tag{62}$$

where we have introduced the new variable

$$u = \frac{1}{y_3}. \tag{63}$$

This change of variables transforms (62) into the new system

$$\begin{aligned} \frac{dy_1}{d\varphi} &= -\frac{5f_l}{7\dot{\varphi}(0)}\frac{1}{u^2} \\ \frac{dy_2}{d\varphi} &= -\frac{5f_l}{7\dot{\varphi}(0)}(\sin\alpha)\frac{1}{u} \\ \frac{d^2u}{d\varphi^2} &= -(1-\tfrac{5}{7}\sin^2\alpha)u + (1-\tfrac{2}{7}\sin\alpha - \tfrac{5}{7}\sin^2\alpha)\frac{1}{{y_1}^2u^2} + \tfrac{2}{7}(\sin\alpha)\frac{y_2}{y_1}\,. \end{aligned} \tag{64}$$

Note that we used relation (25) to eliminate the coefficients g and $R(0)$. Note also that the new set of equations reveals an explicit dependency on only two, dimensionless parameters

$$\varepsilon = \frac{5f_l}{7\dot{\varphi}(0)} \approx 8.8 \times 10^{-3}, \tag{65}$$

and

$$\delta = \sin\alpha \approx 8.3 \times 10^{-2}. \tag{66}$$

The approximate values are based on the measurement results in (35), the estimated value $\widehat{f}_l$ in (60), and the theoretical value of $\dot{\varphi}(0)$ in (37).

The expression in terms of two small parameters tempts us to employ an asymptotic method. To this end, we need an independent variable of magnitude $O(1)$, whereas the current variable φ reaches as far as 160. We therefore define a new variable

$$\phi = \varepsilon\varphi, \tag{67}$$

which is of magnitude $O(1)$. We can now try to expand the solution into an asymptotic power series in δ and ε, with coefficients expressed in terms of ϕ: the powers will indicate the order of the approximation, the coefficients reflect the overall behaviour. The behaviour of the solution is depicted in Fig. 7, showing a smooth downward movement, whereupon superposed a small oscillation. The period of the oscillation appears to be of $O(\varepsilon^{-1})$ when considered as a function of ϕ, and of $O(1)$ when considered as a function of φ. Hence, this process has two different time scales, represented by φ and ϕ. Therefore, it is useful to consider y_1, y_2, and u as functions of both variables φ and ϕ. To this end, we introduce new variables by

$$v(\varphi,\phi) = \frac{1}{y_1},\ w(\varphi,\phi) = y_2,\ u(\varphi,\phi) = u. \tag{68}$$

System (64) now transforms into

$$\begin{aligned}
\frac{\partial v}{\partial \varphi} + \varepsilon\frac{\partial v}{\partial \phi} &= \varepsilon\frac{v^2}{u^2} \\
\frac{\partial w}{\partial \varphi} + \varepsilon\frac{\partial w}{\partial \phi} &= -\delta\varepsilon\frac{1}{u} \\
\frac{\partial^2 u}{\partial \varphi^2} + 2\varepsilon\frac{\partial^2 u}{\partial\varphi\partial\phi} + \varepsilon^2\frac{\partial^2 u}{\partial \phi^2} &= -(1-\tfrac{5}{7}\delta^2)u + (1-\tfrac{2}{7}\delta-\tfrac{5}{7}\delta^2)\frac{v^2}{u^2} + \tfrac{2}{7}\delta v w\,.
\end{aligned} \tag{69}$$

Without loss of generality we furthermore assume that

$$\varphi(0) = \phi(0) = 0, \tag{70}$$

thus transforming the set of initial conditions in (58) into

$$\begin{aligned}
v(0,0) = w(0,0) = u(0,0) &= 1 \\
\frac{\partial u}{\partial \varphi}(0,0) + \varepsilon\frac{\partial u}{\partial \phi}(0,0) &= 0\,.
\end{aligned} \tag{71}$$

We now expand u, v, and w into the following asymptotic power series

$$\begin{aligned}
u &= \textstyle\sum_{i=0}^{m}\delta^i u_i + O(\delta^{m+1}) \\
v &= \textstyle\sum_{i=0}^{m}\delta^i v_i + O(\delta^{m+1}) \\
w &= \textstyle\sum_{i=0}^{m}\delta^i w_i + O(\delta^{m+1})\,,
\end{aligned} \tag{72}$$

with

$$\begin{aligned}
u_i &= \textstyle\sum_{j=0}^{n}\varepsilon^j u_{ij} + O(\varepsilon^{n+1}) \\
v_i &= \textstyle\sum_{j=0}^{n}\varepsilon^j v_{ij} + O(\varepsilon^{n+1}) \\
w_i &= \textstyle\sum_{j=0}^{n}\varepsilon^j w_{ij} + O(\varepsilon^{n+1})\,,\ i = 0,1,\cdots,m\,.
\end{aligned} \tag{73}$$

We shall try to find solutions for u_{ij}, v_{ij}, and w_{ij} - on a limited time scale, where $\phi = O(1)$, $\varphi = O(\varepsilon^{-1})$ - by substituting these power series into (69) and (71), and by matching the corresponding powers $\delta^i \varepsilon^j$. We start by comparing the powers of ε, tentatively neglecting the influence of parameter δ. The equations in (69) thus simplify to

$$\begin{aligned} \frac{\partial v_0}{\partial \varphi} + \varepsilon \frac{\partial v_0}{\partial \phi} &= \varepsilon \frac{{v_0}^2}{{u_0}^2} \\ \frac{\partial w_0}{\partial \varphi} + \varepsilon \frac{\partial w_0}{\partial \phi} &= 0 \\ \frac{\partial^2 u_0}{\partial \varphi^2} + 2\varepsilon \frac{\partial^2 u_0}{\partial \varphi \partial \phi} + \varepsilon^2 \frac{\partial^2 u_0}{\partial \phi^2} &= -u_0 + \frac{{v_0}^2}{{u_0}^2}\,. \end{aligned} \tag{74}$$

The second equation in this system leads - via (71) - to the simple solution

$$w_0 = 1. \tag{75}$$

This leaves us with only two variables, u_0 and v_0, representing the first order approximations of radius R and angular velocity $\dot{\varphi}$. Substitution of power series (73) into the first equation in (74) yields

$$\begin{aligned} 0 = \; & \varepsilon^0 \; [\frac{\partial v_{00}}{\partial \varphi}] + \\ & \varepsilon^1 \; [\frac{\partial v_{01}}{\partial \varphi} + \frac{\partial v_{00}}{\partial \phi} - \frac{{v_{00}}^2}{{u_{00}}^2}] + \\ & \varepsilon^2 \; [\frac{\partial v_{02}}{\partial \varphi} + \frac{\partial v_{01}}{\partial \phi} + \frac{2u_{01}{v_{00}}^2}{{u_{00}}^3} - \frac{2v_{00}v_{01}}{{u_{00}}^2}] + \\ & \varepsilon^3 \; [\frac{\partial v_{03}}{\partial \varphi} + \frac{\partial v_{02}}{\partial \phi} - \frac{3{u_{01}}^2{v_{00}}^2}{{u_{00}}^4} + \frac{2u_{02}{v_{00}}^2}{{u_{00}}^3} + \frac{4u_{01}v_{00}v_{01}}{{u_{00}}^3} - \frac{{v_{01}}^2}{{u_{00}}^2} - \frac{2v_{00}v_{02}}{{u_{00}}^2}] + O(\varepsilon^4), \end{aligned} \tag{76}$$

whereas substitution into (71) yields

$$0 = \varepsilon^0[v_{00}(0,0) - 1] + \varepsilon^1 v_{01}(0,0) + \varepsilon^2 v_{02}(0,0) + \varepsilon^3 v_{03}(0,0) + O(\varepsilon^4). \tag{77}$$

In a similar way we can write out the third equation in (74):

$$\begin{aligned} 0 = \; & \varepsilon^0 \; [\frac{\partial^2 u_{00}}{\partial \varphi^2} + u_{00} - \frac{{v_{00}}^2}{{u_{00}}^2}] + \\ & \varepsilon^1 \; [\frac{\partial^2 u_{01}}{\partial \varphi^2} + 2\frac{\partial^2 u_{00}}{\partial \varphi \partial \phi} + u_{01} + \frac{2u_{01}{v_{00}}^2}{{u_{00}}^3} - \frac{2v_{00}v_{01}}{{u_{00}}^2}] + \\ & \varepsilon^2 \; [\frac{\partial^2 u_{02}}{\partial \varphi^2} + 2\frac{\partial^2 u_{01}}{\partial \varphi \partial \phi} + \frac{\partial^2 u_{00}}{\partial \phi^2} + u_{02} - \frac{3{u_{01}}^2{v_{00}}^2}{{u_{00}}^4} + \frac{2u_{02}{v_{00}}^2}{{u_{00}}^3} + \frac{4u_{01}v_{00}v_{01}}{{u_{00}}^3} - \frac{{v_{01}}^2}{{u_{00}}^2} - \frac{2v_{00}v_{02}}{{u_{00}}^2}] + \\ & \varepsilon^3 \; [\frac{\partial^2 u_{03}}{\partial \varphi^2} + 2\frac{\partial^2 u_{02}}{\partial \varphi \partial \phi} + \frac{\partial^2 u_{01}}{\partial \phi^2} + \frac{4{u_{01}}^3{v_{00}}^2}{{u_{00}}^5} - \frac{6u_{01}u_{02}{v_{00}}^2}{{u_{00}}^4} - \frac{6{u_{01}}^2v_{00}v_{01}}{{u_{00}}^4} + \\ & \frac{4u_{02}v_{00}v_{01}}{{u_{00}}^3} + \frac{2u_{01}{v_{01}}^2}{{u_{00}}^3} + \frac{4u_{01}v_{00}v_{02}}{{u_{00}}^3} - \frac{2v_{01}v_{02}}{{u_{00}}^2}] + O(\varepsilon^4), \end{aligned} \tag{78}$$

with corresponding initial conditions - from (71) -

$$0 = \varepsilon^0[u_{00}(0,0) - 1] + \varepsilon^1 u_{01}(0,0) + \varepsilon^2 u_{02}(0,0) + \varepsilon^3 u_{03}(0,0) + O(\varepsilon^4), \tag{79}$$

and

$$\begin{aligned} 0 = \quad & \varepsilon^0 \quad [\frac{\partial u_{00}}{\partial \varphi}(0,0)] + \varepsilon^1[\frac{\partial u_{01}}{\partial \varphi}(0,0) + \frac{\partial u_{00}}{\partial \phi}(0,0)] + \\ & \varepsilon^2 \quad [\frac{\partial u_{02}}{\partial \varphi}(0,0) + \frac{\partial u_{01}}{\partial \phi}(0,0)] + \varepsilon^3[\frac{\partial u_{03}}{\partial \varphi}(0,0) + \frac{\partial u_{02}}{\partial \phi}(0,0)] + O(\varepsilon^4). \end{aligned} \tag{80}$$

We start by matching the coefficients of ε^0 in (76) and (78), from which we find

$$\begin{aligned} \frac{\partial v_{00}}{\partial \varphi} &= 0 \\ \frac{\partial^2 u_{00}}{\partial \varphi^2} &= -u_{00} + \frac{{v_{00}}^2}{{u_{00}}^2} \,. \end{aligned} \tag{81}$$

The corresponding initial conditions follow from matching the coefficients of ε^0 in (77), (79), and (80):

$$\begin{aligned} v_{00}(0,0) = u_{00}(0,0) &= 1 \\ \frac{\partial u_{00}}{\partial \varphi}(0,0) &= 0 \,. \end{aligned} \tag{82}$$

The solution to these equations is given by

$$v_{00} = V_{00}(\phi), \; u_{00} = \{V_{00}(\phi)\}^{2/3}, \; V_{00}(0) = 1. \tag{83}$$

We proceed with the coefficients of ε^1. Substitution of the solutions for u_{00} and v_{00} into (76) to (80) renders

$$\begin{aligned} \frac{\partial v_{01}}{\partial \varphi} &= -\frac{dV_{00}}{d\phi} + {V_{00}}^{2/3} \\ \frac{\partial^2 u_{01}}{\partial \varphi^2} + 3u_{01} &= 2\frac{v_{01}}{{V_{00}}^{2/3}} \,, \end{aligned} \tag{84}$$

with initial conditions

$$\begin{aligned} u_{01}(0,0) = v_{01}(0,0) &= 0 \\ \frac{\partial u_{01}}{\partial \varphi}(0,0) &= -\tfrac{2}{3} \,. \end{aligned} \tag{85}$$

Since the functions v_{ij} represent coefficients in an asymptotic power series, we know their magnitude to be of $O(1)$. A bounded solution to the first equation (84) can only be acquired if

$$\frac{dV_{00}}{d\phi} = {V_{00}}^{2/3}, \tag{86}$$

which leads - via (83) - to the solutions

$$v_{00} = (1 + \frac{\phi}{3})^3, \; u_{00} = (1 + \frac{\phi}{3})^2. \tag{87}$$

Substitution of these results into system (84) yields

$$\begin{aligned}\frac{\partial v_{01}}{\partial \varphi} &= 0 \\ \frac{\partial^2 u_{01}}{\partial \varphi^2} + 3u_{01} &= 6\frac{v_{01}}{\phi+3}\,,\end{aligned} \tag{88}$$

from which we find

$$v_{01} = V_{01}(\phi),\ u_{01} = \frac{2V_{01}(\phi)}{\phi+3} + A_1(\phi)\sin(\sqrt{3}\varphi) + B_1(\phi)\cos(\sqrt{3}\varphi), \tag{89}$$

with - from the initial conditions in (85) -

$$A_1(0) = -\frac{2}{9}\sqrt{3},\ B_1(0) = 0. \tag{90}$$

The coefficients of ε^2 in (76) and (77) lead to

$$\frac{\partial v_{02}}{\partial \varphi} = -\frac{dV_{01}}{d\phi} + \frac{2V_{01}}{\phi+3} - 2[A_1\sin(\sqrt{3}\varphi) + B_1\cos(\sqrt{3}\varphi)],\ v_{02}(0,0) = 0. \tag{91}$$

The solution remains bounded only if

$$\frac{dV_{01}}{d\phi} = \frac{2V_{01}}{\phi+3}, \tag{92}$$

yielding - with (89) -

$$v_{01} = V_{01} = 0, \tag{93}$$

and

$$v_{02} = V_{02}(\phi) + \frac{2\sqrt{3}}{3}[A_1(\phi)\cos(\sqrt{3}\varphi) - B_1(\phi)\sin(\sqrt{3}\varphi)],\ V_{02}(0) = \frac{4}{9}. \tag{94}$$

Substitution of (93) and (94) into the coefficient of ε^2 in (78) yields

$$\begin{aligned}&\frac{\partial^2 u_{02}}{\partial \varphi^2} + 3u_{02} = \\ &-\frac{2}{9} + \frac{6v_{02}}{\phi+3} + 2\sqrt{3}[(\frac{dB_1}{d\phi} - \frac{2B_1}{\phi+3})\sin(\sqrt{3}\varphi) - (\frac{dA_1}{d\phi} - \frac{2A_1}{\phi+3})\cos(\sqrt{3}\varphi)] + \\ &\frac{27}{2(\phi+3)^2}[(A_1{}^2 + B_1{}^2) + 2A_1B_1\sin(2\sqrt{3}\varphi) + (B_1{}^2 - A_1{}^2)\cos(2\sqrt{3}\varphi)],\end{aligned} \tag{95}$$

which can only lead to a bounded solution if

$$\begin{aligned}\frac{dA_1}{d\phi} - \frac{2A_1}{\phi+3} &= 0 \\ \frac{dB_1}{d\phi} - \frac{2B_1}{\phi+3} &= 0\,.\end{aligned} \tag{96}$$

Combining this result with the initial conditions in (90) renders the solution

$$A_1 = -\frac{2\sqrt{3}}{9}(1+\frac{\phi}{3})^2,\ B_1 = 0, \tag{97}$$

which - with (89) and (93) - leads to

$$u_{01} = -\frac{2\sqrt{3}}{9}(1+\frac{\phi}{3})^2 \sin(\sqrt{3}\varphi). \tag{98}$$

We can continue this process of matching and substitution until we reach a satisfactory level of accuracy, say $O(\varepsilon^3)$. For the corresponding coefficients we thus obtain

$$v_{02} = \frac{2}{81}(1+\frac{\phi}{3})(\phi^2 + 15\phi + 18 - (1+\frac{\phi}{3})\cos(\sqrt{3}\varphi)), \tag{99}$$

$$u_{02} = \frac{2}{81}(\phi^2 + 12\phi + 12 - \frac{\phi^3 + 108\phi + 351}{27}\cos(\sqrt{3}\varphi) + (1+\frac{\phi}{3})^2\cos(2\sqrt{3}\varphi)). \tag{100}$$

Here we finally found an explicit solution to the simplified system in (74). Conclusions are left for the next section.

5 Conclusions

In a deterministic model, the orbit of the ball in the drum is completely determined by the equations of motion, as in (25) and (46). This system of equations can be solved numerically by employing a Runge-Kutta method - as depicted in Figs. 6 to 11 - and part of the solution can even be obtained exactly - as in (59) - through simple calculus. The full system of equations can however not be solved analytically, so we have to recourse to asymptotic methods to approximate the solution to a certain accuracy. The explicit expressions of the solution can be utilized to determine or predict the orbit of the ball, and hence the outcome of the game, but the experimental data from [De Vos 1994] already indicate that a completely deterministic model will not suffice, and random factors will have to be included. Nevertheless, we can draw some interesting conclusions from the results we found so far.

The outcome of the game can be represented by the final angle

$$\varphi_f = \varphi(t_f). \tag{101}$$

The final angle can be computed by substituting the estimated coefficient of air friction from (60) and the observed initial angular velocity from (61) into a Runge-Kutta procedure, as has in fact already been done in Section 4.2. Fig. 14 however shows that this estimated final time is unfit for use. By employing an extended model, we might expect to obtain a better estimate, but we still have to realize that even a small inaccuracy in one of the parameters will lead to an entirely different outcome. Nevertheless it is often claimed that players can make a better than random guess on the outcome by adding the estimated final angle to the angle where the ball leaves the rim. Although this strategy may seem simple and effective, it has several drawbacks, one being the fact that the point of descent is very hard to determine by mere observation.

A more manageable prediction method might emerge from the asymptotic results in Section 4.3. There we found an explicit expression for variable u_0, which - according to

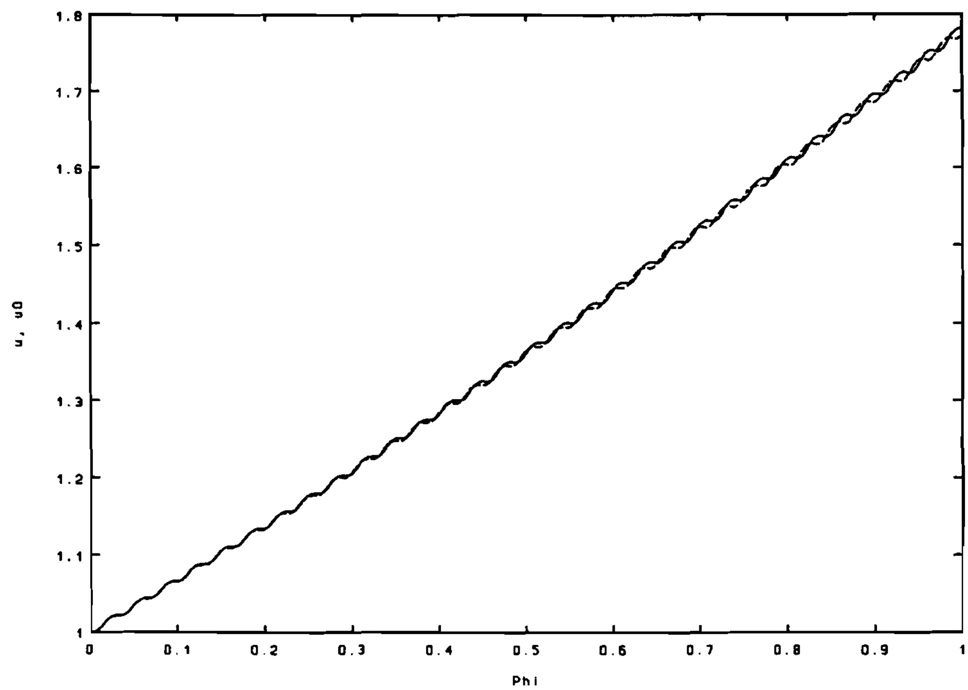

Figure 15: Variable u_0 compared to variable u

(56), (63) and (72) - roughly coincides with the reciprocal of radius R. From equation (98) we can deduce

$$\begin{aligned} {u_0}^2 &= (1+\frac{\phi}{3})^4\{1-\frac{4\varepsilon\sqrt{3}}{9}\sin(\sqrt{3}\varphi)\}+O(\varepsilon^2) \\ &= (1+\frac{\phi}{3})^4\{1+\frac{4\varepsilon\sqrt{3}}{9}\cos(\sqrt{3}(\varphi+\frac{\pi\sqrt{3}}{6}))\}+O(\varepsilon^2), \end{aligned} \tag{102}$$

which - particularly the part between the braces - strongly resembles the phase plane equation of an ordinary ellipse:

$$\frac{2a^2b^2}{\rho^2}=(b^2+a^2)+(b^2-a^2)\cos(2\varphi). \tag{103}$$

Apart from a decaying factor $(1+\frac{\phi}{3})^4$, the expression of ${u_0}^2$ in (102) represents an elliptical curve with an ellipticity of $1-\frac{2}{9}\sqrt{3}\varepsilon+O(\varepsilon^2)$. Since u_0 is apparently periodic with period $2\pi/\sqrt{3}$, the orientation of the elliptical curve varies with φ. If u_0 would exactly represent the reciprocal of radius R, then any of its observed minima - or maxima - could be used to extrapolate to the next or to the previous minimum, and thus to the position where the ball left the rim, or even to where it will fall down in the numbered ring. Major drawbacks of this strategy are that u_0 does not exactly represent the reciprocal of R, and that the ball does not necessarily have to fall down at one of the curve's minima.

Since the pattern of rotating ellipses is quite easy to observe, it could provide a helpful mechanism for predicting the outcome of the game. For an accurate prediction algorithm we obviously need accurate approximations, but here we still have to cope with an error of $O(\delta)$. Fig. 15 compares u_0 (which is represented by the dashed line) to the numerical results for $u=R_0/R$. The most remarkable difference is a change in periodicity, which must be caused by neglecting the influence of parameter δ. These δ-effects will have to be determined through future research; because of the shifting periodicity, we believe that the Poincaré-Linstedt method will eventually lead to a fitting asymptotic power series. From the supplemental asymptotic results we will be able to derive some practical rules of thumb, which will allow players to predict the outcome of a deterministic game. Nevertheless, a prediction strategy for Golden Ten will not be available until we have extended our deterministic model with some random factors; the nature of these factors will have to be determined through matching the deterministic solution to experimental data, as provided by [De Vos 1994].

References

[De Vos 1994] De Vos, J.C., *A Thousand Golden Ten Orbits,* Report FEW 654, Tilburg University, The Netherlands.